

PRESTACK DEPTH MIGRATION USING STRAIGHT RAY TECHNIQUE (SRT)

HARRY Y. LIM¹, DONG-JOO MIN², CHANGSOO SHIN¹, DONGWOO YANG¹,
YOUNGHO CHA¹ and JUNG HEE SUH¹

¹ School of Civil, Urban and Geosystem Engineering, Seoul National University, San 56-1, Shillim-dong, Kwanak-ku, Seoul 151-742, Korea.

² Korea Ocean Research and Development Institute, Ansan, P.O. Box 29, Kyungki 425-600, Korea.

(Received March 26, 2001; revised version accepted April 16, 2002)

ABSTRACT

Lim, H.Y., Min, D.-J., Shin, C.-S., Yang, D.-W., Cha, Y. and Suh, J.H., 2002. Prestack depth migration using straight ray technique (SRT). *Journal of Seismic Exploration*, 11: 271-281.

Kirchhoff prestack depth migration requires an elaborate book-keeping effort and a massive IO process to construct Kirchhoff hyperbolas. In order to avoid the complexity of the programming code and the massive IO process, we propose a straight ray technique (SRT) for traveltimes calculations in Kirchhoff migration. Since all the rays are straight in polar coordinates for the 2D velocity model, or in spherical coordinates for the 3D velocity model, traveltimes can be simply computed along a straight ray for a given source-receiver configuration, without suffering from shadow zones and caustics, and used directly for building Kirchhoff hyperbolas. In this way, we circumvent the substantial IO process required for reading traveltimes on a disk and save computational storage. Numerical examples demonstrate that SRT computes traveltimes intermediate between first-arrival traveltimes and the most energetic arrival traveltimes, resulting in better images than the first arrival traveltimes for the 2D IFP Marmousi data. With the implementation of SRT for 2D Kirchhoff migration, we successfully extend our SRT to 3D Kirchhoff migration for the SEG/EAGE salt dome data.

KEY WORDS: straight ray technique, Kirchhoff prestack depth migration, traveltimes calculation, Kirchhoff hyperbola, polar coordinate, spherical coordinate.

INTRODUCTION

Kirchhoff prestack depth migration needs a single traveltimes and amplitude from a source to a depth point in the subsurface as an asymptotic Green's function of the wave equation. For calculating the traveltimes needed in seismic imaging and velocity analysis, ray-based methods and finite-difference eikonal equation solvers have been widely used.

Ray-based methods (Cassell, 1982; Červený et al., 1977; Um and Thurber, 1987) accurately compute traveltimes for multiple arrivals, but sometimes suffer from large shadow zones and interpolation problems. Finite-difference eikonal solvers, which avoid these problem, have proven to be unconditionally stable (Vidale, 1988; Qin et al., 1990; van Trier and Symes, 1991; Podvin and Lecomte, 1991; Popovici, 1991a, 1991b; Cao and Greenhalgh, 1994; Schneider, 1995; Sethian and Popovici, 1999). However, finite-difference eikonal solvers only compute the first-arrival traveltimes, which often miss the most energetic wave event.

Geoltrain et al. (1993) and Nichols (1996) asserted that the most energetic arrival traveltimes provide higher fidelity images than the first-arrival traveltimes. Although there are several methods of calculating the most energetic arrival traveltimes using either ray-based methods (e.g., the Gaussian beam method; Hill, 1990) or wave equation solutions (Nichols, 1996), unfortunately it is difficult and expensive to compute the most energetic arrival traveltimes.

In Kirchhoff prestack depth migration, we often store the computed traveltimes and field data on disk, and then read them from the disk to construct Kirchhoff hyperbola. As a result, the complexity of Kirchhoff prestack depth migration algorithm is mainly dependent upon how to load the computed traveltimes stored on disk into computer memory and how to minimize the IO process of reading traveltimes.

In this paper, we propose a SRT that does not require the writing of traveltimes on a disk and loading them into computer memory for Kirchhoff migration. SRT has been used in prestack time migration, even though it is not supported theoretically. We begin by supporting the theoretical basis of SRT and then give numerical examples for the IFP Marmousi and 3D SEG/EAGE salt dome models.

STRAIGHT RAY TECHNIQUE AND THE VELOCITY MODEL TRANSFORM

To provide a theoretical base for SRT, we design SRT in polar and spherical coordinates for 2D and 3D, respectively. Although we only describe 2D SRT in polar coordinates, extension of our algorithm to 3D SRT is straightforward.

For our SRT, we first define a polar coordinate system having an origin at a source point as shown in Fig.1. We also assume that within a cell of Fig.1, slowness is constant along an arc, but varies linearly in a radial direction. In the coordinate system, we note that all the rays are shot in radial directions and that all the raypaths are straight even though material properties change as the rays propagate in radial directions. As a result, we can easily compute traveltimes on straight rays from a source to a depth in the subsurface. In the SRT, we can also calculate amplitude simply by applying a transmission coefficient relationship between a layered cake model and geometrical spreading.

Since velocity models are given in the Cartesian coordinate, the next step performed in SRT is to transform a velocity model in Cartesian coordinate into a velocity model in polar coordinates. For the transform of the velocity model, we use interpolation algorithms, such as the bilinear and bi-cubic algorithms. In Fig. 2, we display an original four-layer velocity model in Cartesian coordinate and three angular velocity models transformed into the polar coordinates with different polar cell divisions. Fig. 2 shows that the coarse cell division greatly distorts the velocity model, and as the grid spacing approaches zero ($\Delta r \rightarrow 0$ and $\Delta \theta \rightarrow 0$), the transformed velocity model approaches the original model. From these results, we note that errors in traveltimes computed using SRT mainly come from differences between the original in the Cartesian coordinate and the transformed velocity model in polar coordinates.

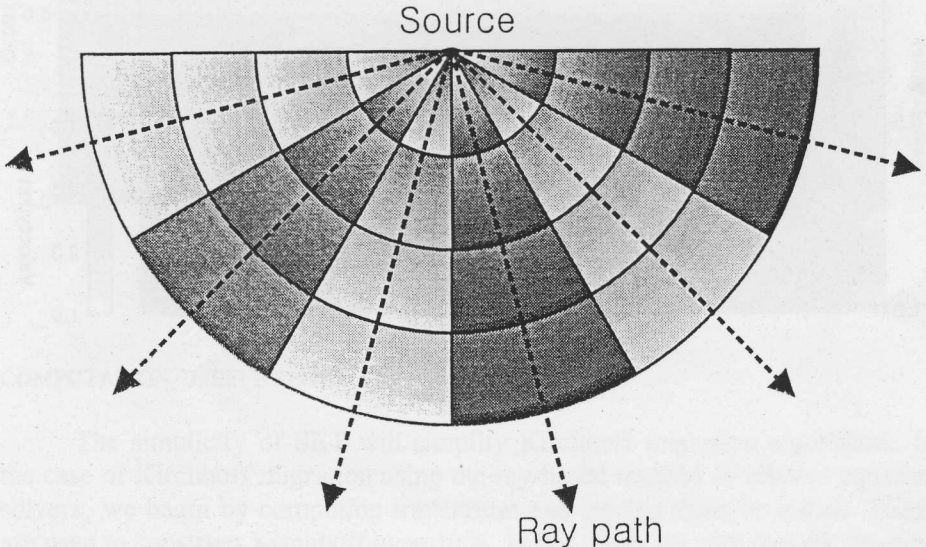
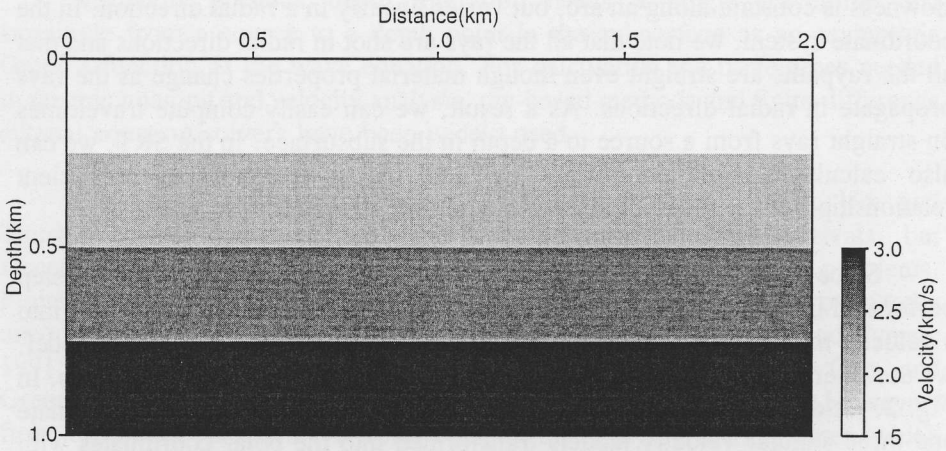
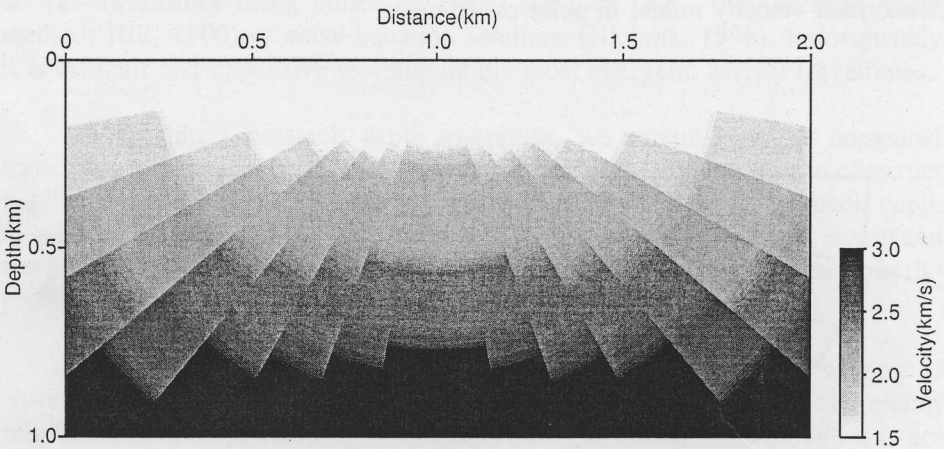


Fig. 1. A polar coordinate for SRT.

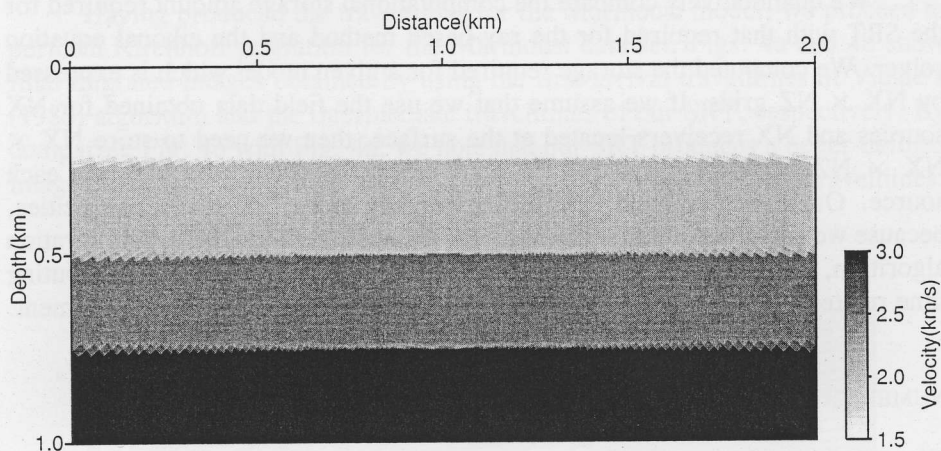


(a)

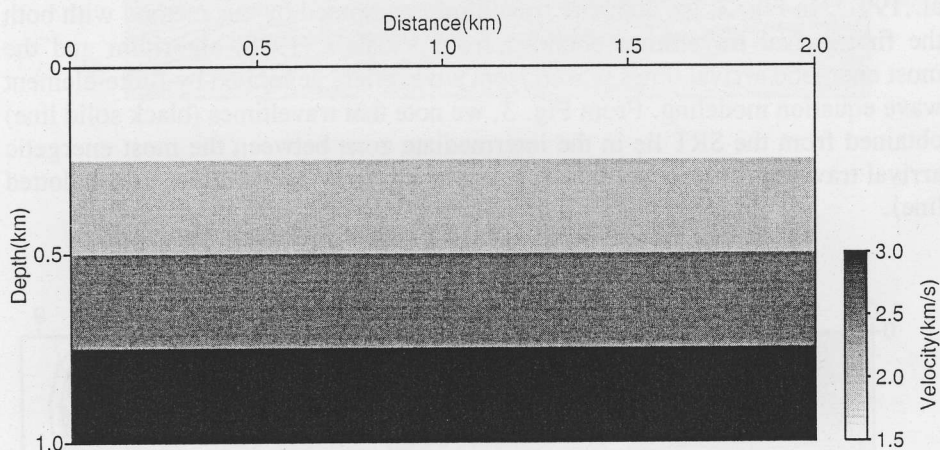


(b)

Fig. 2. Comparison of model discretization errors for a four-layered model where velocities are 1500, 2000, 2500 and 3000 m/s, respectively: (a) original velocity model in a Cartesian coordinate, (b) transformed velocity model with $\Delta r = 70$ m and $\Delta\theta = 10^\circ$, (c) transformed velocity model with $\Delta r = 7$ m and $\Delta\theta = 1^\circ$, and (d) transformed velocity model with $\Delta r = 0.7$ m and $\Delta\theta = 0.1^\circ$.



(c)



(d)

COMPUTATIONAL EFFICIENCY

The simplicity of SRT will simplify Kirchhoff migration algorithms. In the case of Kirchhoff migration using the ray-based method or eikonal equation solvers, we begin by computing traveltimes and storing them on a disk. These are used to construct Kirchhoff hyperbola. In this case, we note that the massive IO process required results in congestion in a popular PC-based cluster machine. However, in our SRT we avoid massive IO process by computing traveltimes and then using them directly in Kirchhoff migration algorithm.

We quantitatively compare the computational storage amount required for the SRT with that required for the ray-based method and the eikonal equation solver. We computed the storage required for a given model which is expressed by $NX \times NZ$ grids. If we assume that we use the field data obtained for NX sources and NX receivers located at the surface, then we need to store $NX \times NX \times NZ$ traveltimes and $NX \times NZ$ velocity model on the disk for each source. On the other hand, for SRT, we only store $NX \times NZ$ velocities, because we can compute traveltimes on-the-fly, use them in Kirchhoff migration algorithm, and then discard them. In this way, we also reduce the computing time related to the IO process in addition to computational storage requirement.

NUMERICAL EXAMPLES

The IFP Marmousi model

To ensure that the SRT gives a good migrated image for a complex model, we applied our SRT algorithm to the Marmousi data set (Bourgeois et al., 1991). In Fig. 3, we compare traveltimes computed by our method with both the first-arrival traveltimes obtained from Vidale's (1988) algorithm and the most energetic arrival times picked from a wavefield generated by finite-element wave equation modeling. From Fig. 3, we note that traveltimes (black solid line) obtained from the SRT lie in the intermediate zone between the most energetic arrival traveltimes (white solid line) and the first-arrival traveltimes (black dotted line).

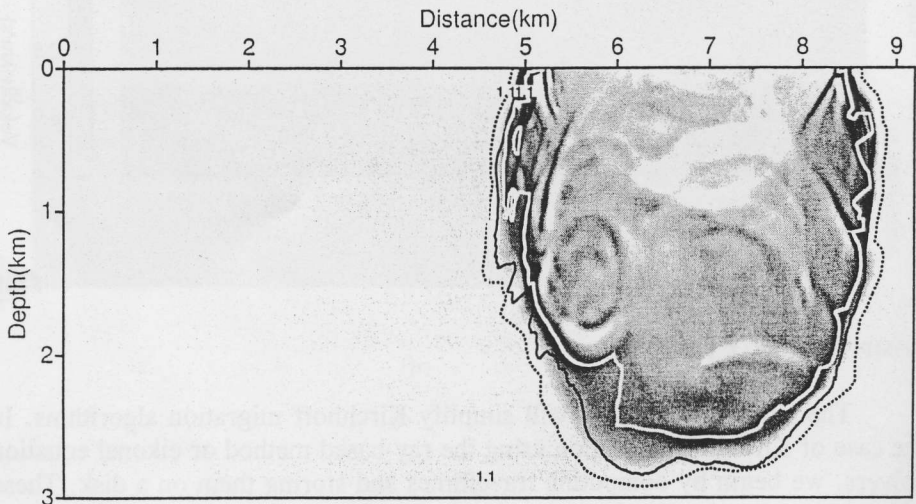
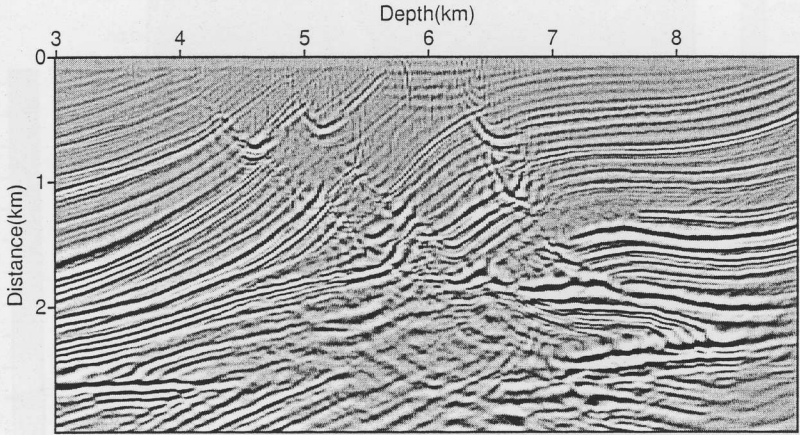
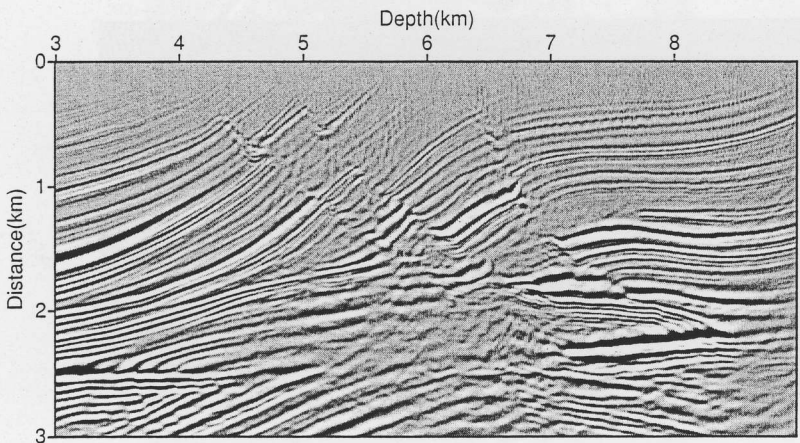


Fig. 3. Traveltimes computed by SRT (black solid line), first arrival traveltimes by Vidale's (1988) algorithm (black dashed line) and the most energetic arrival traveltimes picked from the wavefields by FEM modeling (white solid line) overlaid on a snapshot image obtained by FEM modeling.

Having produced the traveltimes for the Marmousi model, we proceed to perform Kirchhoff migration for the Marmousi data set. Figs. 4a and 4b show final migrated images obtained by using the first-arrival traveltimes of Vidale's (1988) algorithm and the intermediate traveltimes of our SRT, respectively. By comparing Fig. 4b with Fig. 4a, we note that our SRT produces a better-defined image of the fault boundaries and the reservoir than Vidale's (1988) traveltimes.



(a)



(b)

Fig. 4. Migrated images produced using (a) first arrival traveltimes by Vidale's (1988) algorithm and (b) traveltimes by SRT.

The SEG/EAGE Salt dome model

We also apply SRT to the 3D SEG/EAGE salt dome model. The overall model size is $13.5 \times 13.5 \times 4.2$ km, and the grid interval 20 m. Fig. 5a shows traveltimes contours computed by SRT overlaid on an inline section at $x = 7220$ km, and Fig. 5b shows a corresponding migrated image. We note that the final, migrated image obtained using our SRT has good agreement with the original model. Well-imaged layer boundaries and fault lines are apparent.

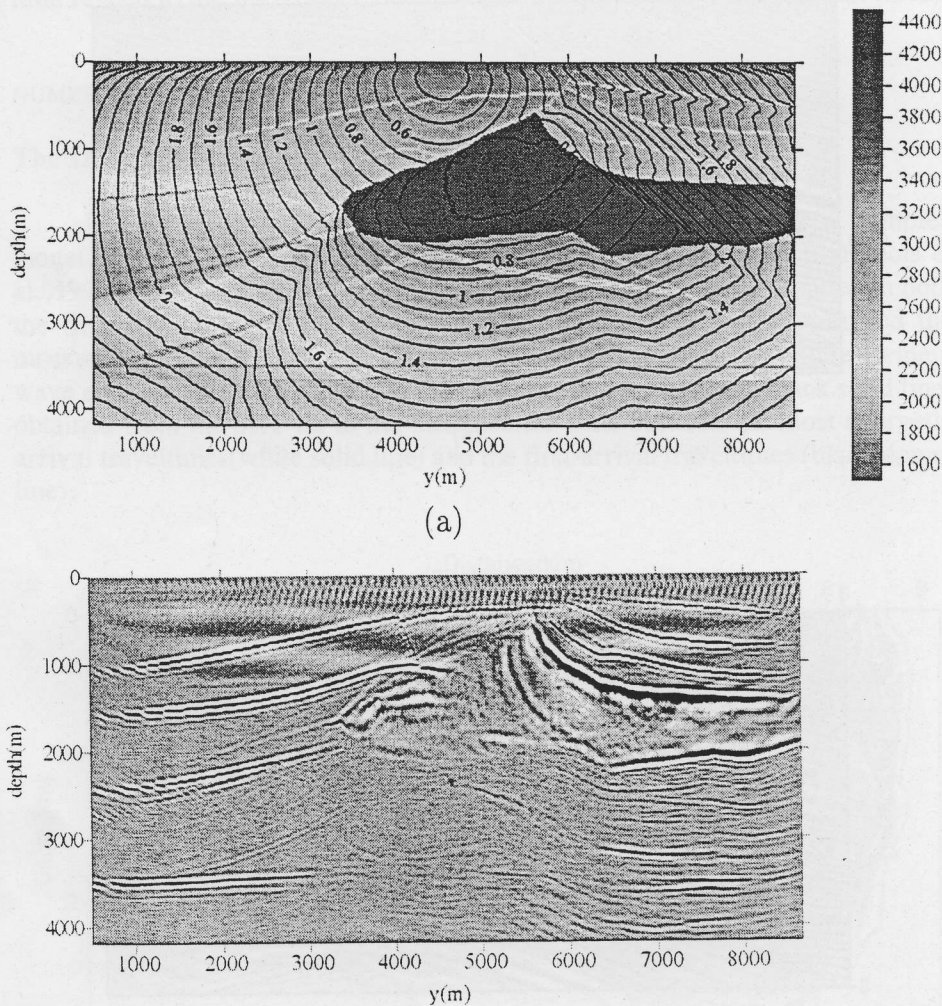
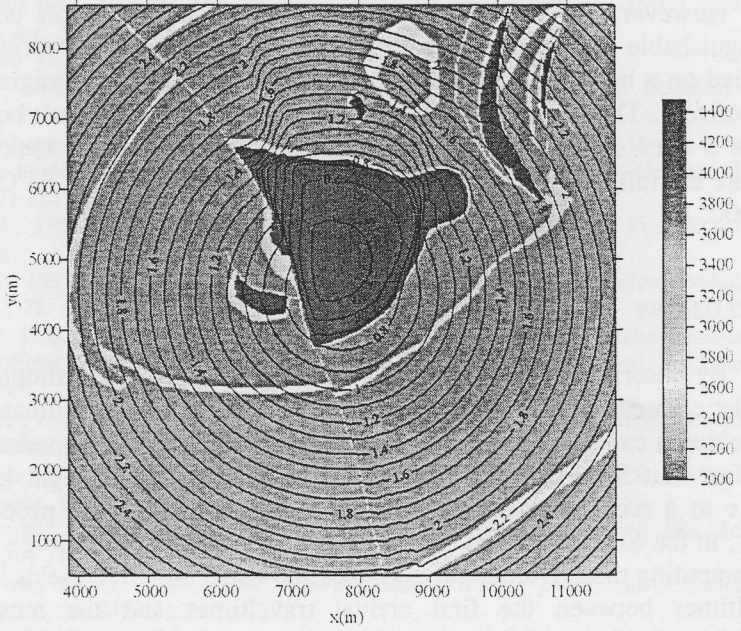


Fig. 5. (a) Traveltime contours generated by SRT and (b) migrated image at $x = 7440$ m for the 3D SEG/EAGE salt dome model.



(a)

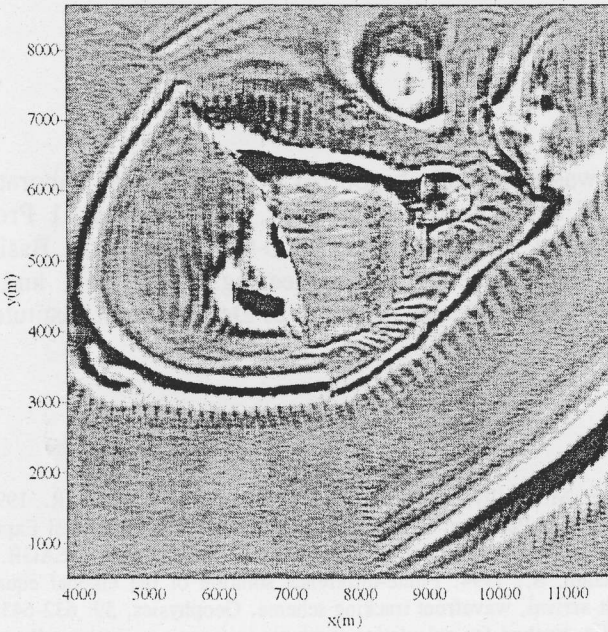


Fig. 6. (a) Traveltime contours generated by SRT and (b) migrated image at $z = 1240$ m for the 3D SEG/EAEG salt dome model.

However, most of the layer boundaries under the salt body are not distinguishable on the section. Figs. 6a and 6b show traveltimes contours overlaid on a horizontal slice at a depth of 1240 m and their migration image, respectively. The horizontal slice cuts the central part of the salt body. Fig. 6b shows a very clear image of the complex salt boundary. It took 4 hours to migrate the full data set with the traveltimes of the SRT using 64 CPUs of IBM RS6000.

CONCLUSIONS

By describing SRT in polar coordinates, we present a simple traveltimes calculation method. Since all the rays are straight in polar coordinates, our SRT has neither a caustic problem nor the shadow zone for complex velocity models. The fact that SRT directly computes traveltimes along straight lines from a source to a receiver makes it possible to avoid massive IO processes. As a result, in the SRT migration algorithm, we reduce both the storage amount and the computing time. Numerical examples show that our SRT yields intermediate traveltimes between the first arrival traveltimes and the most energetic traveltimes, and that the intermediate traveltimes give better images than the first-arrival traveltimes by Vidale's (1988) algorithm. By applying SRT to the 3D SEG/EAGE salt dome model, we show that SRT can be successfully extended to 3D velocity model.

ACKNOWLEDGEMENT

This work was financially supported by the National Laboratory Project of the Ministry of Science and Technology, Brain Korea 21 Project of the Ministry of Education, grant No. R05-2000-00003 from the Basic Research Program of the Korea Science & Engineering Foundation, and grant No. PM10300 from the Korea Ocean Research & Development Institute.

REFERENCES

- Bourgeois, A., Bourget, M., Lailly, P., Poulet, M., Ricarte, P. and Versteeg, R., 1991. Marmousi, model and data. In: Bersteeg, R. and Grau, G. (Eds.), *The Marmousi Experience*. Proc. 1990 EAGE workshop on Practical Aspects of Seismic Data Inversion. EAGE, Bunnik: 5-16.
- Cao, S. and Greenhalgh, S., 1994. Finite-difference solution of the eikonal equation using an efficient, first-arrival, wavefront tracking scheme. *Geophysics*, 59: 632-643.
- Cassell, B.R., 1982. A method for calculating synthetic seismograms in laterally varying media. *Geophys. J. R. Astr. Soc.*, 38: 9-19.
- Červený, V., Molotkov, I.A. and Psencik, I., 1977. *Ray Method in Seismology*. Univ. of Karlova Press, Prague.

- Geoltrain, S. and Brac, J., 1993. Can we image complex structures with first-arrival traveltimes? *Geophysics*, 58: 564-575.
- Hill, N.R., 1990. Gaussian beam migration. *Geophysics*, 55: 1416-1428.
- Nichols, D.E., 1996. Maximum energy traveltimes calculated in the seismic frequency band. *Geophysics*, 61: 253-263.
- Podvin, P. and Lecomte, I., 1991. Finite-difference computation of traveltimes in very contrasted velocity models: A massively parallel approach and its associated tools. *Geophys. J. Int.*, 105: 271-284.
- Popovici, A.M., 1991a. Finite-difference traveltimes maps. Stanford Explor. Proj. Report, 70: 245-256.
- Popovici, A.M., 1991b. Stability of finite-difference traveltimes algorithms. Stanford Explor. Proj. Report., 72: 135-138.
- Qin, F., Olsen, K.B., Luo, Y. and Schuster, G.T., 1990. Solution of the eikonal equation by a finite-difference method. Expanded Abstr., 60th Ann. Internat. SEG Mtg., San Francisco: 1004-1007.
- Schneider, W.A., Jr., 1995. Robust and efficient upwind finite-difference traveltimes calculations in three dimensions. *Geophysics*, 60: 1108-1117.
- Sethian, J.A. and Popovici, A.M., 1999. 3D traveltimes computation using the fast marching method. *Geophysics*, 64: 516-523.
- Um, J. and Thurber, C., 1987. A fast algorithm for two-point seismic ray tracing. *Bull. Seismol. Soc. Am.*, 77: 972-986.
- van Trier, J. and Symes, W.W., 1991. Upwind finite-difference calculation of traveltimes. *Geophysics*, 56: 812-821.
- Vidale, J.E., 1988. Finite-difference calculation of traveltimes. *Bull. Seismol. Soc. Am.*, 78: 2062-2076.